





Multisite NHERF1 phosphorylation controls GRK6A regulation of hormone-sensitive phosphate transport

Received for publication, December 7, 2020, and in revised form, February 22, 2021. Published, Papers in Press, February 24, 2021.
<https://doi.org/10.1016/j.jbc.2021.100473>

Maria Vistrup-Parry¹, W. Bruce Sneddon², Sofie Bach¹, Kristian Strømgaard¹, Peter A. Friedman² , and Tatyana Mamonova^{2,*} 

From the ¹Center for Biopharmaceuticals, Department of Drug Design and Pharmacology, University of Copenhagen, Copenhagen, Denmark; and ²Laboratory for GPCR Biology, Department of Pharmacology and Chemical Biology, University of Pittsburgh School of Medicine, Pittsburgh, Pennsylvania, USA

Edited by Mike Shipston

The type II sodium-dependent phosphate cotransporter (NPT2A) mediates renal phosphate uptake. The NPT2A is regulated by parathyroid hormone (PTH) and fibroblast growth factor 23, which requires Na⁺/H⁺ exchange regulatory factor-1 (NHERF1), a multidomain PDZ-containing phosphoprotein. Phosphocycling controls the association between NHERF1 and the NPT2A. Here, we characterize the critical involvement of G protein-coupled receptor kinase 6A (GRK6A) in mediating PTH-sensitive phosphate transport by targeted phosphorylation coupled with NHERF1 conformational rearrangement, which in turn allows phosphorylation at a secondary site. GRK6A, through its carboxy-terminal PDZ recognition motif, binds NHERF1 PDZ1 with greater affinity than PDZ2. However, the association between NHERF1 PDZ2 and GRK6A is necessary for PTH action. Ser¹⁶², a PKCα phosphorylation site in PDZ2, regulates the binding affinity between PDZ2 and GRK6A. Substitution of Ser¹⁶² with alanine (S¹⁶²A) blocks the PTH action but does not disrupt the interaction between NHERF1 and the NPT2A. Replacement of Ser¹⁶² with aspartic acid (S¹⁶²D) abrogates the interaction between NHERF1 and the NPT2A and concurrently PTH action. We used amber codon suppression to generate a phosphorylated Ser¹⁶²(pSer¹⁶²)-PDZ2 variant. *K_D* values determined by fluorescence anisotropy indicate that incorporation of pSer¹⁶² increased the binding affinity to the carboxy terminus of GRK6A 2-fold compared with WT PDZ2. Molecular dynamics simulations predict formation of an electrostatic network between pSer¹⁶² and Asp¹⁸³ of PDZ2 and Arg at position -1 of the GRK6A PDZ-binding motif. Our results suggest that PDZ2 plays a regulatory role in PTH-sensitive NPT2A-mediated phosphate transport and phosphorylation of Ser¹⁶² in PDZ2 modulates the interaction with GRK6A.

cells (2, 3). NHERF1 tethers potential binding partners through tandem PDZ domains named for the common structural domain shared by the postsynaptic density protein, *Drosophila* disc large tumor suppressor, and zonula occludens-1 protein, and the carboxy-terminal (C-terminal) ezrin-binding domain (EBD) associated with ezrin (4). The association between NHERF1 and the type II sodium-dependent phosphate cotransporter (NPT2A) (*SLC34A1*), the primary renal Na-dependent phosphate transporter, is required for hormone-regulated phosphate transport mediated by the NPT2A (4). Loss-of-function mutations in NHERF1 or the NPT2A disrupt phosphate metabolism and lead to hypophosphatemia (5–7). Parathyroid hormone (PTH) and fibroblast growth factor 23 downregulate the NPT2A–NHERF1 binary complex by activating two distinct signaling pathways that converge at NHERF1 (8–11).

NHERF1 PDZ1 and PDZ2 domains have similar sequences and identical core-binding motifs (-GYGF-) essential for PDZ-ligand interactions (12, 13). NHERF1 PDZ1 and PDZ2 bind the target-sequence of ligand partners through a short C-terminal linear interaction fragment that is three to four residues in length (X-S/T-X-Φ_{COO}⁻ class I PDZ-recognition motifs, where X is any amino acid and Φ is a hydrophobic residue) (14). By convention, these residues are numbered starting from the last position (P⁰) and going backward to P⁻¹, P⁻², P⁻³, and so forth.

Prior experimental studies revealed that G protein-coupled receptor kinase 6A (GRK6A) possessing a canonical PDZ ligand motif (-TRL⁵⁷⁶) at its C terminus binds NHERF1 PDZ domains (15). Most binding is associated with PDZ1. However, a minor interaction between GRK6A and the PDZ2 domain is critical for constitutive or PTH-induced phosphorylation of NHERF1 at Ser²⁹⁰ (15, 16) and for PTH-sensitive phosphate transport (16). The biological puzzle is how does PDZ2 become accessible to GRK6A and what is the role of PTH in this process. Solving this dilemma is the goal of this study. We hypothesized that enzymatic phosphorylation of Ser¹⁶² located adjacent to the PDZ2 core-binding motif (-¹⁶³GYGF¹⁶⁶-) and incorporation of a double-charged phosphate group promote association between PDZ2 and GRK6A. Ser¹⁶² is a defined PKCα phosphorylation site (17, 18). Notably, PKC is a major pathway of PTH signaling (19–21) and is the only PKC isoform

Na⁺/H⁺ exchange regulatory factor-1, NHERF1 (*SLC9A3R1*), also known as the ezrin-binding phosphoprotein of 50 kDa, belongs to the NHERF family (1) and is the only known PDZ-containing scaffold that controls protein localization at the apical plasma membrane of polarized epithelial

* For correspondence: Tatyana Mamonova, tbm7@pitt.edu.

Phosphoserine 162 of PDZ2 orchestrates binding to GRK6A

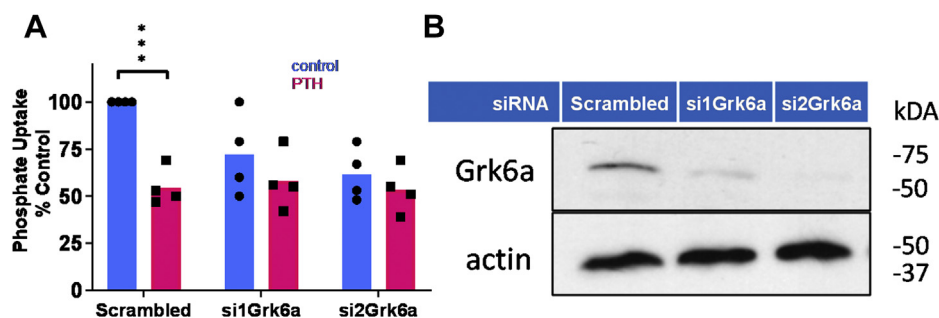


Figure 1. Grk6a knockdown eliminates PTH-sensitive phosphate uptake. A, Grk6a expression was inhibited by siRNAs targeted to opossum Grk6a (si1Grk6a, si2Grk6a). Phosphate uptake was measured in opossum kidney (OK) cells as described in [Experimental procedures](#). Results report the mean \pm SD ($n = 4$; $***p < 0.001$, ANOVA); B, confirmation of Grk6a knockdown was assessed by immunoblot and compared with β -actin from the same samples. si1GRK6A and si2GRK6A reduced GRK6A expression by 90% and 98%, respectively, as compared with cells transfected with Scrambled siRNA ($n = 2$). GRK6A, G protein-coupled receptor kinase 6A; PTH, parathyroid hormone.

with a PDZ-recognition motif at its C terminus (-SAV⁶⁷²) (22, 23). It remains to be established whether the interaction between NHERF1 and PKC α is necessary for phosphorylation of Ser¹⁶².

The experiments described here use a variety of complementary approaches to characterize the role of PDZ2 with phosphodeficient Ser¹⁶² on NHERF1-dependent PTH-sensitive phosphate uptake. Binding determinants of the interaction between PDZ2 or PDZ2 with phospho-Ser¹⁶², introduced genetically in NHERF1 using amber codon suppression, for the first time, and GRK6A were evaluated using fluorescence anisotropy (FA) and confirmed by molecular dynamics (MD) simulations. Our preliminary study suggests that a double-charged phospho-Ser¹⁶² is a key determinant of PTH signaling and is required for NHERF1-dependent NPT2A-mediated PTH-sensitive phosphate uptake.

Results

Direct interaction between NHERF1 and GRK6A is essential for NPT2A-mediated PTH-sensitive phosphate transport

We first tested whether GRK6A is required for PTH-inhibitable phosphate uptake. For these experiments, we used opossum kidney (OK) cells that constitutively express Npt2a, Nherf1, and Grk6a and are considered the definitive model for PTH-sensitive phosphate transport[†]. Grk6a was knocked down with targeted siRNA constructs. Both siRNA1 and siRNA2 reduced the response to PTH in the treated cells (Fig. 1A). si1Grk6a and si2Grk6a both reduced Grk6a expression by 90% and 98%, respectively (Fig. 1B). This finding implicates Grk6a in PTH-mediated signaling and regulation of Npt2a function.

We next examined whether NHERF1 coimmunoprecipitates with Grk6a. Opossum kidney clone H (OKH) cells, functionally deficient in Nherf1 (24), were transfected with Flag-NHERF1 (WT) or Flag-NHERF1 constructs where the PDZ core-binding site -GYGF- was mutated to (-GAGA-) in PDZ1 (N1P1-GAGA), PDZ2 (N1P2-GAGA), or both (N1P1P2-GAGA). GRK6A more strongly interacts with N1P2-GAGA

than with N1P1-GAGA (Fig. 2, A and B) (15). The nature of the high molecular weight band (>75 kDa) (Fig. 2A), which is not present in host cells, is not known. The binding affinity between recombinant NHERF1, N1P1-GAGA, or N1P2-GAGA constructs was determined by FA using a FITC-labeled 22-residue C-terminal GRK6A peptide (-⁵⁵³QRLFSRQDCCGNCSEELPTRL⁵⁷⁶ [GRK6Act-22]) (Table 1). The findings reinforce the coimmunoprecipitation results (Fig. 2A). Full-length NHERF1 and NHERF1 with the modified PDZ2 (N1P2-GAGA) interact with a FITC-labeled human GRK6A C-terminal 22 amino acid peptide, GRK6Act-22, with dissociation constants (K_D) of $5.3 \pm 0.7 \mu\text{M}$ and $3.6 \pm 0.2 \mu\text{M}$, respectively. The interaction between full-length NHERF1 with the modified PDZ1 (N1P1-GAGA) and GRK6Act-22, is much less evident (Fig. S1, blue curve). To rule out the possibility of an effect of NHERF1 self-association on the K_D , we additionally measured K_D for an N1P1-GAGA construct wherein the C terminus ³⁵⁵-FSNL³⁵⁸ was mutated to ⁻³⁵⁵AAAA³⁵⁸ ($\Delta 4$). Only a modest effect was observed on the binding between N1P1-GAGA $\Delta 4$ and GRK6Act-22 (Fig. S1, green curve). However, deleting the NHERF1 C-terminal (Δ EBD, 326–358 aa) substantially increased binding affinity (Fig. S1, red curve). The observed effect on affinity corroborates earlier studies showing that the flexible C-terminal EBD of NHERF1 limits access of cystic fibrosis transmembrane conductance regulator (CFTR) (-TRL ligand) to PDZ domains (18).

Next, we probed if N1P2-GAGA interacts with GRK6A to support PTH action on phosphate uptake. To accomplish this, we used OKH cells transfected with N1P2-GAGA and treated with 100 nM PTH(1–34). WT NHERF1 and N1P1-GAGA were used as positive and negative controls, respectively. Surprisingly, N1P2-GAGA, like WT NHERF1, supports PTH inhibition of phosphate transport (Fig. 3). These findings imply that despite the modified PDZ2 core-binding motif in N1P2-GAGA, Grk6a nonetheless is able to interact with PDZ2, leading to phosphorylation of Ser²⁹⁰ and PTH action. How, then, might Grk6a bind PDZ2 with a disrupted core-binding motif?

Insofar as N1P2-GAGA with the altered PDZ core-binding motif (-¹⁶³GYGF¹⁶⁶-) is denied a canonical interaction with the Grk6a C-terminal PDZ-ligand motif (-TRL), we sought to

[†] Human proteins are indicated by three-letter uppercase convention; genes in italics. Only the first letter is uppercase for the corresponding nonhuman protein or gene.

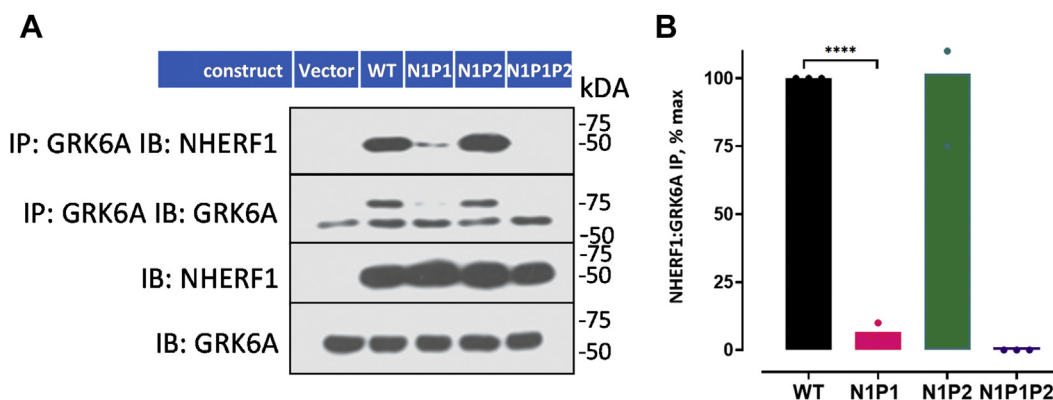


Figure 2. GRK6A binds PDZ1-NHERF1 under resting conditions. A, representative immunoblot of NHERF1:GRK6A coIP. HA-GRK6A was cotransfected with either empty vector or the indicated FLAG-NHERF1 construct into OKH cells. WT-NHERF1 coimmunoprecipitates with GRK6A, as does N1P2-GAGA-NHERF1 (PDZ1 intact). N1P1-GAGA (PDZ2 intact) and N1P1P2-GAGA/GAGA (both PDZ domains are modified) do not interact with NHERF1. B, NHERF1 coIP with GRK6A was quantified in transfected OKH cells and normalized to WT-NHERF1 (100%). N1P2 interacts with GRK6A to a similar extent to WT-NHERF1. Disruption of PDZ1 (N1P1-GAGA, N1P1P2-GAGA/GAGA) eliminated binding of GRK6A. Results report the mean \pm SD ($n = 3$; **** $p < 0.0001$, ANOVA). coIP, coimmunoprecipitation; GRK6A, G protein-coupled receptor kinase 6A; NHERF1, Na⁺/H⁺ exchange regulatory factor-1.

determine which residues in N1P2-GAGA support binding with Grk6a. We reasoned that the appearance of phospho-Ser¹⁶² flanking the PDZ2 core-binding motif (-¹⁶³GYGF¹⁶⁶-) and known as a direct substrate of PKC α (17, 18) might augment binding of PDZ2 with the -TRL motif of Grk6a.

Effect of Ser¹⁶² on PTH-sensitive phosphate transport

To investigate the effect of Ser¹⁶² phosphorylation on PTH-sensitive phosphate transport, we generated NHERF1 constructs wherein Ser¹⁶² was replaced by Ala (phosphoresistant mutant) or by Asp (phosphomimetic mutant). The phosphomimetic S¹⁶²D mutation resulted in a significant reduction of basal phosphate transport compared with WT NHERF1 (Fig. 4), reflecting the absence of an interaction between Npt2a and NHERF1 S¹⁶²D. In contrast, the phospho-resistant S¹⁶²A mutant did not affect basal phosphate transport but somewhat abrogated the inhibitory response to PTH compared with WT NHERF1 (Fig. 4). Representative immunoblots demonstrate that the S¹⁶²A mutant associates with Npt2a, whereas S¹⁶²D failed to coimmunoprecipitate with Npt2a (Fig. 5). These results suggest that phosphomimetic S¹⁶²D may restrict the interaction between NHERF1 PDZ1 and Npt2a.

Phospho-Ser¹⁶² increases association between PDZ2 and GRK6A

To explore further the role of Ser¹⁶² on GRK6A binding phosphorylated Ser¹⁶² (hereafter pSer¹⁶²), was genetically

Table 1

Binding affinities between full-length NHERF1 or NHERF1 constructs and GRK6Act-22

NHERF1 construct	K_D , μM^a
WT NHERF1	5.3 \pm 0.7
N1P2-GAGA	3.6 \pm 0.2
N1P1-GAGA	>100

FA, fluorescence anisotropy; GRK6Act-22, -⁵⁵³QLFRSQDCCGNCSEELPTRL⁵⁷⁶; NHERF1, Na⁺/H⁺ exchange regulatory factor-1.

^a Dissociation constants (K_D s) were derived from the three independent FA experiments performed in triplicate. The means and SD are given ($n = 3$; **** $p < 0.0001$, ANOVA).

introduced in a recombinant PDZ2 (133–300) using amber codon suppression (25). Previously, semisynthesis was effectively applied to generate site-specific phosphorylated PDZ domains (26). Here, we used amber codon suppression to genetically encode pSer at position 162, which in the future will allow us to access phosphorylated full-length proteins comprising PDZ domains. This strategy requires a unique aminoacyl synthetase and tRNA pair specific for pSer and orthogonal to the natural translation system of *Escherichia coli*, thereby preventing cross-reactivity (25). Upon induction with IPTG, pSer was site-specifically incorporated into PDZ2 at position 162. The introduction of pSer was characterized as a mass change of 80 Da corresponding to the phosphate group as determined by LC-MS (Fig. S2). The secondary structure of the protein was measured by CD (Fig. S2).

The binding affinity between pSer¹⁶²-PDZ2 (133–300 aa) and FITC-labeled GRK6Act-22 was determined by FA and

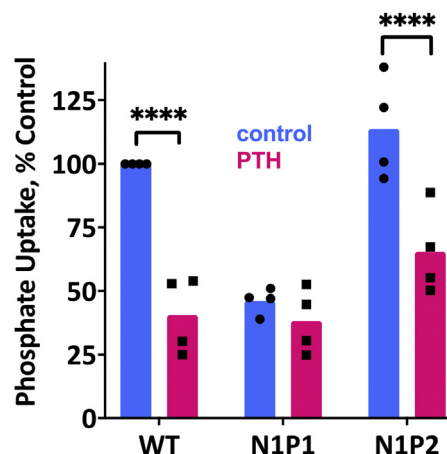


Figure 3. Effect of NHERF1 PDZ mutants on basal and PTH-sensitive phosphate uptake. OKH cells were transiently transfected with WT-NHERF1, N1P1-GAGA, or N1P2-GAGA. Cells were treated with vehicle or with 100 nM PTH(1–34). N1P2-GAGA-NHERF1 and WT-NHERF1 support PTH-inhibitable phosphate uptake, whereas N1P1-GAGA does not. Results report the mean \pm SD ($n = 4$; **** $p < 0.0001$, ANOVA). NHERF1, Na⁺/H⁺ exchange regulatory factor-1; PTH, parathyroid hormone.

Phosphoserine 162 of PDZ2 orchestrates binding to GRK6A

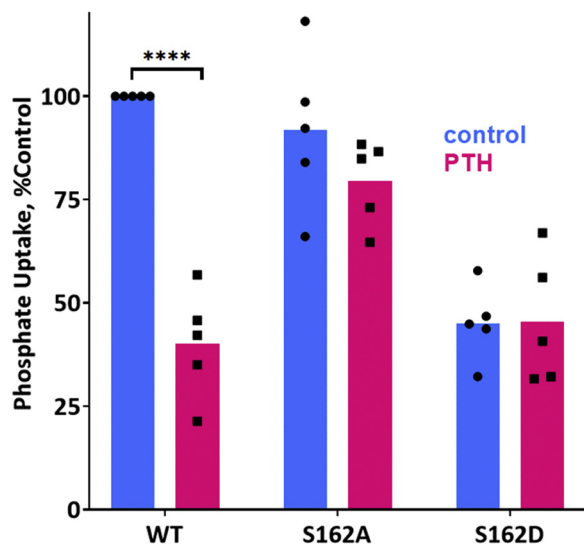


Figure 4. Ser¹⁶² is essential for PTH-inhibitable phosphate uptake. OKH cells were transiently transfected with WT-NHERF1 or with S¹⁶²A-NHERF1 or S¹⁶²D-NHERF1. Cells were treated with vehicle or with 100 nM PTH(1–34). Results report the mean \pm SD ($n = 4$; **** $p < 0.0001$, ANOVA). NHERF1, Na⁺/H⁺ exchange regulatory factor-1; PTH, parathyroid hormone.

compared with the WT PDZ2 domain (133–300 aa) and S¹⁶²A-PDZ2 (133–300 aa) (Table 2). The results demonstrate that the K_D values for the interaction between WT PDZ2 or S¹⁶²A-PDZ2 and GRK6Act-22 were comparable (51.3 ± 0.4 , $43.4 \pm 0.4 \mu\text{M}$) and 2-fold higher than for pSer¹⁶²-PDZ2 (26.1 ± 0.8 ; $p < 0.0001$ ANOVA) (Table 2 and Fig. S3). Thus, pSer¹⁶²-PDZ2 enhanced binding affinity for GRK6A.

Computational prediction of NHERF1 and GRK6A binding determinants

We then applied explicit-solvent MD simulation to explore the structural determinants underlying the binding specificity of NHERF1 PDZ domains for GRK6A. A 9-residue, C-terminal GRK6A peptide (⁻⁵⁶⁸SEEELPTRL⁵⁷⁶) was used. The complexes between PDZ1, PDZ2, or pSer¹⁶²-PDZ2 and a 9-residue, C-terminal GRK6A peptide (⁻⁵⁶⁸SEEELPTRL⁵⁷⁶) were

Table 2

Binding affinities between isolated PDZ2 domain or PDZ2 mutants and GRK6Act-22

PDZ2 construct	K_D , μM
WT PDZ2	51.3 ± 0.7^a
pSer ¹⁶² -PDZ2	26.1 ± 0.8^b
S ¹⁶² A-PDZ2	43.4 ± 0.4^a

FA, fluorescence anisotropy; GRK6Act-22, ⁻⁵⁵³QRLFSRQDCCGNCSEEELPTRL⁵⁷⁶; pSer¹⁶², phosphorylated Ser¹⁶².

Phosphorylated design is indicated by “p”. FA experiments were performed in triplicate.

^a Means and SDs are given ($n = 3$; **** $p < 0.0001$, ANOVA).

^b Means and SDs are given ($n = 5$; **** $p < 0.0001$, ANOVA).

computationally generated with the docking program ZDOCK (27) as described in Experimental procedures. The docking structures (Fig. S4) demonstrate that the C terminus of GRK6A (^{-T⁻²R⁻¹L⁰}) goes deep in the PDZ1 or PDZ2 hydrophobic cavity between the $\alpha 2$ helix and the $\beta 2$ sheet. The ^{-TRL} motif is involved in canonical interactions with the conserved residues from the core-binding motif ²³GYGF²⁶, $\alpha 2$ (Val⁷⁶, Arg⁸⁰), $\beta 2$ (Leu²⁸), or ¹⁶³GYGF¹⁶⁶, Val²¹⁶, Arg²²⁰, Leu¹⁶⁸ of PDZ1 and PDZ2, respectively. His⁷² or His²¹² of PDZ1 and PDZ2, respectively, specifically target Thr⁻² of GRK6A. The PDZ2–GRK6Act-9 peptide (⁻⁵⁶⁸SEEELPTRL⁵⁷⁶) (hereafter GRK6Act-9) complex, in contrast to PDZ1–GRK6A, was unstable and showed a tendency to dissociate after 130 ns of MD simulation. MD simulations predict that in addition to the canonical PDZ-ligand interactions, Glu⁴³ of PDZ1 associates tightly with the positively charged side chain of Arg⁻¹ of GRK6A. The short distance (less than 2 Å) between the carboxylate oxygens of Glu⁴³ (O ϵ^1 and O ϵ^2) and the NH η^2 group of Arg⁻¹ of GRK6A permits formation of strong electrostatic interactions (Fig. S4A). Compared with Glu⁴³, Asp¹⁸³ at the homologous position in PDZ2 does not interact with the side chain of Arg⁻¹. The latter is solvent-exposed and characterized by multiple orientations during the MD simulation. The distances between the NH η^2 group of Arg⁻¹ and carboxylate oxygens of Asp¹⁸³ (O δ^1 and O δ^2) from 6.8 to 13.4 Å along the simulation time trajectory (Fig. S4B) indicate that the naturally occurring Glu to Asp replacement on PDZ2 decreases the binding affinity for the C-terminal motif of

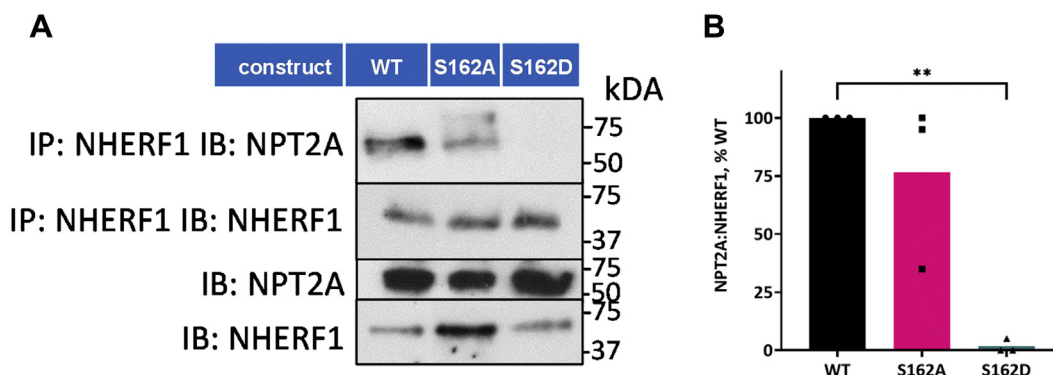


Figure 5. S¹⁶²D phosphomimetic mutation disrupts the interaction between NHERF1 and NPT2A. A, about 293 cells were transfected with HA-NPT2A and the indicated form of FLAG-NHERF1 (WT, S¹⁶²A, S162D). Phosphoresistant S¹⁶²A coimmunoprecipitated with NHERF1 nearly as robustly as WT. Notably, the S¹⁶²D phosphomimetic ablated the interaction with NPT2A ($n = 1$). Identical results were observed with OKH cells transfected with HA-GFP-NPT2A and FLAG-NHERF1 (WT, S¹⁶²A, S162D) ($n = 2$). B, the summary of quantified IP results from (A). Results were normalized to WT-NHERF1 (100%) and report the mean \pm SD ($n = 3$; ** $p < 0.01$, ANOVA). NHERF1, Na⁺/H⁺ exchange regulatory factor-1.

Phosphoserine 162 of PDZ2 orchestrates binding to GRK6A

GRK6A. This observation is consistent with coimmunoprecipitation (Fig. 2) and FA experimental data (Table 1 and Fig. S1) showing a weak association between PDZ2 and GRK6A compared with PDZ1. A similar tendency was observed for NHERF1 PDZ domains interacting with the C-terminal -TRL motif of NPT2A (28) or the C-terminal -TRL motif of CFTR (29–31).

MD simulations demonstrate that incorporation of phospho-Ser¹⁶² does not induce conformational changes in the PDZ2–GRK6Act-9 structure. However, comparative analysis of PDZ2–GRK6Act-9 and pSer¹⁶²–PDZ2–GRK6Act-9 revealed a significant difference in the orientation of Arg⁻¹ of the GRK6A -TRL motif (Fig. 6 and Fig. S4). The positively charged side chain of Arg⁻¹ rotates toward the negatively charged phosphate group of Ser¹⁶² during the first 2 ns of MD simulation and remains in this conformation for the remainder of the simulation (159 ns) (Fig. 6). The average distances calculated between the NH η^1 or NH η^2 group of Arg⁻¹ of GRK6A and OP1 or OP2 group of pSer¹⁶² are around 2 Å for the last 10 ns of MD simulation (Fig. 6). This indicates that the negatively charged phosphate group has a significant impact on dynamics and conformation of the positively charged side chain of Arg⁻¹. Remarkably, the side chain of Asp¹⁸³ changes its orientation and moves toward the side chain of Arg⁻¹. The average distances calculated between the NH η^2 group of Arg⁻¹ of GRK6A and the carboxylate oxygens of Asp¹⁸³ (O δ^1 and O δ^2) of pSer¹⁶²-PDZ2 for the last 10 ns of MD simulation (2.2 Å and 2.9 Å, respectively) (Fig. S5) suggest a strong

stabilizing effect of phospho-Ser¹⁶² on the electrostatic interaction of Arg⁻¹ with Asp¹⁸³. We further computationally substituted Tyr¹⁶⁴ and Phe¹⁶⁶ to Ala in the carboxylate-binding site of pSer¹⁶²-PDZ2. MD simulations (100 ns) demonstrate that the N-terminal part of the GRK6Act-9 peptide is solvent-exposed and faces out of the binding cavity. However, the extreme C terminus and the side chain of Arg⁻¹ of GRK6Act-9 remains in the same conformation as observed for pSer¹⁶²-PDZ2 (Fig. S6). Substitution of Tyr¹⁶⁴ and Phe¹⁶⁶ by Ala disrupts the hydrophobic network formed by side chains of Tyr¹⁶⁴, Phe¹⁶⁶, and Leu⁰ but does not disrupt interactions between backbone amides (NH) of Tyr¹⁶⁴Ala, Gly¹⁶⁵, and Phe¹⁶⁶Ala and C-terminal oxygens of Leu⁰ or a hydrogen bond between His²¹² and Thr⁻² (Figs. 6 and S6). MD simulations predict that the positively charged side chain of Arg⁻¹ is in a dynamic equilibrium between the two negatively charged side chains, pSer¹⁶² and Asp¹⁸³. Thus, pSer¹⁶² has a significant electrostatic impact on the stabilization of the side chain of Arg⁻¹ and the formation of the pSer¹⁶²-Arg⁻¹-Asp¹⁸³ network (Figs. 6 and S6).

Discussion

Although NHERF1 PDZ domains are very similar, they have a distinct ligand specificity. NHERF1 PDZ1 interacts with the type-2 sodium-phosphate cotransporter NPT2A (*SLC34A1*) (32, 33) via C-terminal PDZ-ligand motif (-TRL⁶³⁹). This association is required for hormone-regulated phosphate transport and proper localization of

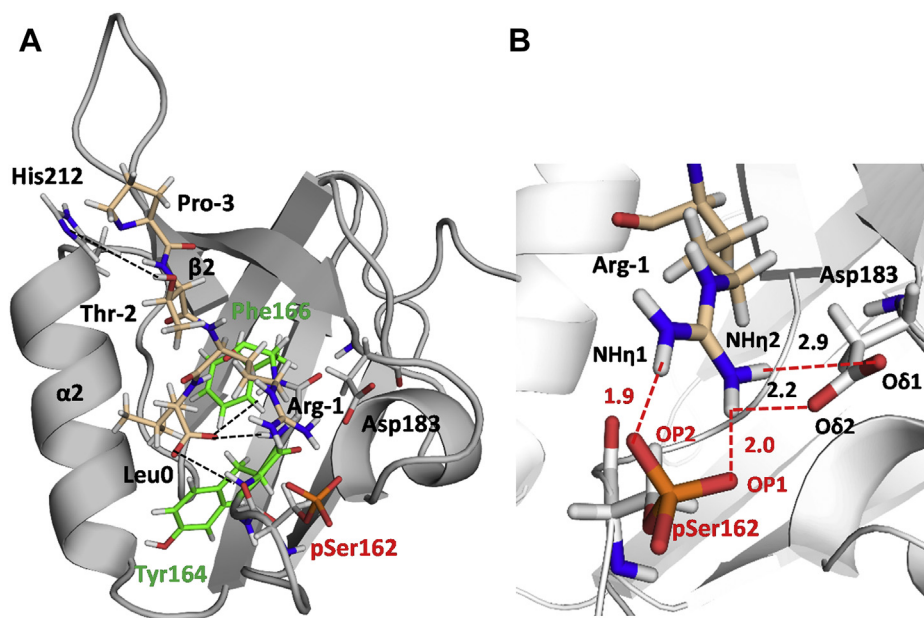


Figure 6. Computational model of pSer¹⁶²-PDZ2 bound to the GRK6Act-9 peptide. The PDZ2 domain is highlighted in gray cartoon, whereas the GRK6Act-9 peptide is represented in wheat sticks. A, the extreme C terminus of GRK6Act-9 ($-P^{-3}T^{-2}R^{-1}L^0$) is inserted in the binding pocket of pSer¹⁶²-PDZ2 between the $\alpha 2$ helix and the $\beta 2$ sheet. Tyr¹⁶⁴ and Phe¹⁶⁶ forming the hydrophobic pocket are shown as green sticks. Hydrogen bonds between the backbone amide (NH) of Tyr¹⁶⁴, Gly¹⁶⁵, and Phe¹⁶⁶ and C-terminal oxygens of Leu⁰ and between His²¹² and Thr⁻² are shown as black dotted lines. The five residues from the N-terminal end of the GRK6Act-9 peptide are facing outside of the PDZ-binding pocket and omitted for simplicity. B, the plausible electrostatic network involved pSer¹⁶²-Arg⁻¹-Asp¹⁸³ is shown as red dotted lines. Average distances between OP1 of pSer¹⁶² and NH η^1 of Arg⁻¹ or between OP2 and NH η^2 are 2.0 Å and 1.9 Å, respectively and between NH η^1 of Arg⁻¹ and O δ^1 or O δ^2 of Asp¹⁸³ are 2.9 Å and 2.2 Å, respectively. Distances were calculated along the last 10 ns of MD simulation. Hydrogen atoms are white, oxygen atoms are red, and nitrogen atoms are blue. GRK6Act-9, ⁻⁵⁶⁸SEELPTRL⁵⁷⁶.

Phosphoserine 162 of PDZ2 orchestrates binding to GRK6A

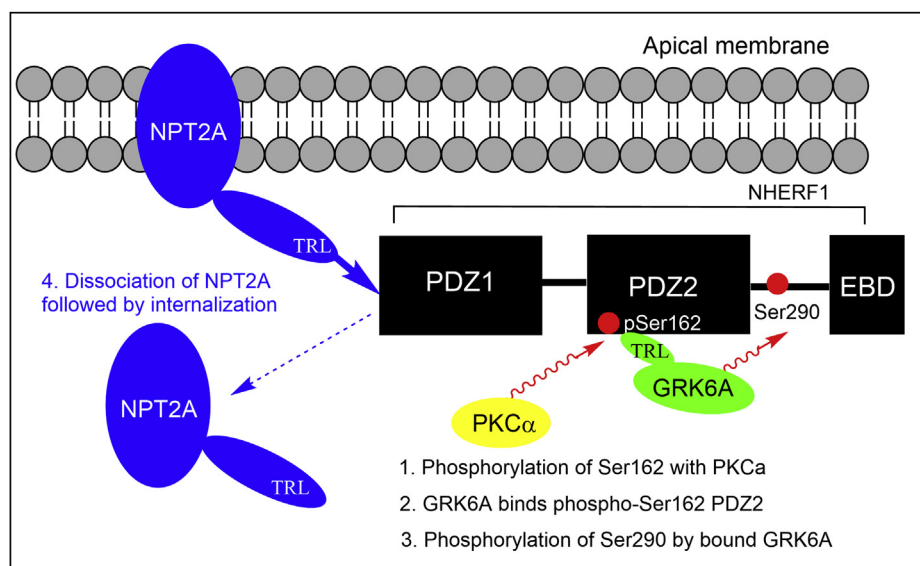


Figure 7. General scheme represents the order of events along NHERF1-dependent PTH-sensitive phosphate uptake. NHERF1 PDZ1 binds NPT2A through the C-terminal (-TRL) motif and that keeps NPT2A at the apical membrane. PTH-induced phosphorylation promotes phosphorylation of Ser¹⁶² by PKC α . GRK6A binds pSer¹⁶²-PDZ2 through the C-terminal (-TRL) motif and phosphorylates Ser²⁹⁰. NPT2A dissociates from NHERF1 and internalizes. GRK6A, G protein-coupled receptor kinase 6A; NHERF1, Na⁺/H⁺ exchange regulatory factor-1; PTH, parathyroid hormone.

NPT2A at the apical membrane (Fig. 7). Previously, we and others showed that the specificity of the interaction between NHERF1 and target ligands harboring Arg⁻¹ at C terminus depend on Glu⁴³ of PDZ1 (12, 28, 31, 34). Glu⁴³ coordinates the interaction with Arg⁻¹ of the C-terminal recognition motif of NPT2A (-T⁻²R⁻¹L⁰) and establishes the strong electrostatic network required for hormone-sensitive phosphate transport (4, 28). Asp¹⁸³ located at the homologous position in PDZ2 is shorter than Glu⁴³. The current MD simulations, prior study (28), and available NMR structure (31) demonstrate that the side chain of Asp¹⁸³ is flexible and not involved in a stable interaction with Arg⁻¹. The Glu⁴³Asp mutation in PDZ1 leads to dramatic loss in affinity with the similar C-terminal -TRL motif of CFTR (31). Consistently, an Asp¹⁸³Glu rescue mutation in PDZ2 restores the electrostatic network between Asp¹⁸³Glu and Arg⁻¹ specific for PDZ1 and significantly increases the binding affinity of PDZ2 (28).

In the present study, we show that knocking down Grk6a by siRNA or si2RNA blocks Npt2a-dependent phosphate uptake in response to PTH (Fig. 1). This observation indicates that GRK6A is an essential regulatory component of NPT2A-dependent PTH-sensitive phosphate transport and corroborates previous findings that GRK6A pharmacological inhibitors abolish PTH action (16). Our data agree with an earlier study demonstrating that NHERF1 is constitutively phosphorylated at Ser²⁹⁰ (35). As expected, siRNA-GRK6A-treated cells do not support basal phosphate uptake (Fig. 1). GRK6A, similar to NPT2A, associates with NHERF1 PDZ domains via the C-terminal PDZ-ligand motif (-TRL). Compatible binding affinities (3 μ M to 5 μ M) were observed for NHERF1-GRK6Act-22 (Table 1) and NHERF1-NPT2Act-22 (28) association. NHERF1 is highly concentrated at apical membranes (8). The concentration of

NHERF1 [P] is in great excess over total membrane-delimited NPT2A [Nt] or GRK6A [Gt]. At the condition when [P] \gg [Nt] and [P] \gg [Gt], equations for the equilibrium binding are as follows:

$$[PG] = [P] \times [Gt] / K_{D2} + [P] \quad (1)$$

$$[PN] = [P] \times [Nt] / K_{D1} + [P] \quad (2)$$

Where [PG], [P], [Gt], [PN], and [Nt] are the concentrations of PDZ1-GRK6A, PDZ1, GRK6A (total), PDZ1-NPT2A, and NPT2A (total), respectively. K_{D1} and K_{D2} are dissociation constants for the PDZ1-GRK6A and PDZ1-NPT2A complexes, respectively. These equations were solved by dividing both sides of Equation 1 by Equation 2. Assuming that $K_{D1} \sim K_{D2}$ yields $[PG]/[PN] = [Gt]/[Nt]$. When [Nt] \gg [Gt], then $[PG]/[PN] \rightarrow 0$. When [P] $\rightarrow \infty$, PDZ1 occupancy will be determined by the total concentration of NPT2A [Nt] although NPT2Act-22 (28) and GRK6Act-22 have similar binding affinities for PDZ1 (Table S1).

The observed weak interaction between isolated PDZ2 and GRK6Act-22 ($K_D = 51.3 \mu$ M in Table 2), as previously reported (15), is consistent with data obtained for PDZ2 in full-length NHERF1 (N1P1-GAGA in Fig. 2A and Table 1). However, this interaction is physiologically relevant and obligatory for the constitutive cellular (15), PTH-induced phosphorylation of Ser²⁹⁰ in NHERF1 (Fig. 7), and NHERF1-dependent PTH-sensitive phosphate transport (16). Generally, the interaction between the carboxylate-binding site of the PDZ domain and the C-terminal residues of the target ligand control binding. To characterize functional and molecular details of the interaction between PDZ2 and GRK6A, we mutated Tyr¹⁶⁴ and

Phe¹⁶⁶ to Ala in the carboxylate-binding loop of NHERF1 (GYGF→GAGA). Published studies established that substitution of bulk hydrophobic residues (Tyr, Phe, Ile, or Leu) in the carboxylate binding loop of PDZ domains by Ala disrupts the hydrophobic network, making PDZ-ligand interactions very weak and frequently unrecognized (4, 20, 36, 37). Mutation of core-binding Tyr¹⁶⁴ and Phe¹⁶⁶ in NHERF1 PDZ2 (N1P2-GAGA) decreased but did not block phosphate transport in response to PTH (Fig. 3). This finding strongly suggests that the PDZ2 domain retains its ability to interact with the C terminus of GRK6A *in vivo*. This raised the hypothesis that unrecognized binding determinants might stabilize the association between PDZ2 and GRK6A. Analysis of residues that may contribute to the binding pointed to Ser¹⁶², known as a PKC α phosphorylation site in human NHERF1 (Fig. 7) (17, 18). Notably, NHERF1 homologs (mouse, rabbit) harbor asparagine at the corresponding position. PKC α action is unique for PDZ2 inasmuch as PDZ1 has Asn²² at the homologous position. The latter may affect PDZ1 binding affinity (12). Ser¹⁶² at the corresponding position of PDZ2 also may stabilize Arg⁻¹ through backbone interactions (38). In this instance, replacement of Ser¹⁶² by Ala would not be expected to alter the binding affinity between PDZ2 and the C terminus of GRK6A as reported here (Table 2). The current results suggest that introducing the double negatively charged phosphate group at Ser¹⁶² increases the binding affinity between PDZ2 and GRK6A (Table 2). Nonetheless, it is not intuitive that the effect of pSer¹⁶² on binding is sufficient albeit relatively minor. One possible explanation is that pSer¹⁶²-PDZ2 was generated and purified using a different protocol compared with recombinant WT or S¹⁶²A-PDZ2. Experimental conditions (buffer, concentration, incubation time, titration) can affect FA measurements. The binding affinity was determined for the isolated PDZ2 domain bound a relatively short (22 aa) C-terminal peptide of GRK6A. We speculate that binding determinants beyond the C-terminal motif of GRK6A may also contribute and stabilize the interaction with full-length NHERF1 *in vivo*. Overall, biochemical experiments support the view that Ser¹⁶² is required for regulation of NPT2A-mediated hormone-sensitive phosphate transport, and specificity of the PDZ2 domain for GRK6A is not determined by the conserved subset of residues (Tyr¹⁶⁴ and Phe¹⁶⁶) but rather specific pSer¹⁶². This finding corroborated with our prior studies demonstrated that a small change in the free energy of binding characterizes PDZ-ligand specificity and is attributed to the enthalpy–entropy compensation (28, 39).

We further reasoned that phosphoresistant NHERF1 S¹⁶²A should reduce PTH action and phosphate transport (Fig. 4). The partial inhibition of PTH-sensitive phosphate transport (Fig. 4) relates to constitutive phosphorylation of Ser²⁹⁰ (15, 16). This observation is compatible with prior work showing that the low binding between the PDZ2 K¹⁵⁸A-K¹⁵⁹A mutant and Grk6a concurrently lowers Ser²⁹⁰ phosphorylation (15). In accord with this finding, S¹⁶²A diminishes the amount of GRK6A bound to NHERF1 and decreases phosphate uptake (Fig. 4). As anticipated, the phosphoresistant S¹⁶²A substitution does not impede the interaction between NHERF1 and

NPT2A (Fig. 5). Surprisingly, phosphomimetic NHERF1 S¹⁶²D did not coimmunoprecipitate with NPT2A (Fig. 5) and suppressed PTH action (Fig. 4). Intriguingly, a similar tendency was observed for Nherf1 Ser⁷⁷ and Thr⁹⁵ phosphorylation sites located in PDZ1 (40). S⁷⁷D blocks interaction with Npt2a and basal phosphate uptake, whereas T⁹⁵A inhibits PTH-sensitive phosphate transport. We speculate that replacement of OH-Ser¹⁶² by COOH-S¹⁶²D causes a conformational reorganization of NHERF1 and, in particular, in the linker segments connecting PDZ1 and PDZ2 (112–146 aa) and PDZ2 and the EBD (252–358 aa), resulting in an NHERF1 conformation that inhibits association between PDZ1 and NPT2A, thereby terminating PTH action.

The biochemical data provided here indicate that the binding affinity of PDZ2 is regulated by phosphorylation of Ser¹⁶² (Table 2). MD simulations complement and provide additional details about the interaction between pSer¹⁶²-PDZ2 and the -T⁻²R⁻¹L⁰ motif of GRK6A. The side chain of Arg⁻¹ emerged rapidly with the negatively charged phosphate group of Ser¹⁶². The side chain of Asp¹⁸³, facing the bulk water in PDZ2, was rotated toward Arg⁻¹ in pSer¹⁶²-PDZ2. The MD simulation demonstrates that introducing the phosphate group faithfully mimics enzymatic phosphorylation and promotes local conformational changes. The formation of an electrostatic network of pSer¹⁶²-Arg⁻¹-Asp¹⁸³ is vital for stabilizing the pSer¹⁶²-PDZ2-GRK6A complex (Table 2 and Fig. S3). This observation is entirely compatible and consistent with our earlier studies that underlined a limited contribution of Asp¹⁸³ on the binding with the C-terminal -TRL motif of NPT2A (28). The C-terminal -TRL motif is not unique. CFTR with the same C-terminal -TRL motif (29, 41) as GRK6A and NPT2A is another natural partner of NHERF1 (42). A recently published X-ray structure complemented by MD simulations (50 ns) demonstrate that Arg⁻¹ of CFTR can form a salt bridge with Asp¹⁸³-PDZ2 (38). However, much longer MD simulation is required to estimate dynamics of this interaction. Further crystallization of NHERF1 PDZ domains with the C-terminal -TRL motif of NPT2A is necessary to distinguish binding determinants and improve our understanding of NHERF1 PDZ-ligand specificity.

Site-specific incorporation of pSer¹⁶² applied here for NHERF1 PDZ2 introduces an analogous but not identical functional group compared with phosphomimetic mutagenesis. The phosphate group has a -2 negative charge compared with the single negative charge of the Asp carboxylate group. The bulkier phosphate group compared with the carboxylate group may importantly perturb the local protein structure (43). This observation underscores the limitation and potential hazard of using phosphomimetics to draw conclusions about phosphorylation and demonstrates the strength of site-specific introduction of pSer using amber codon suppression. Together, these ensemble factors are critical for identifying protein–ligand interactions *in vitro*. Rearrangement of an electrostatic network in pSer¹⁶²-PDZ2 and changes in side chain dynamics may allosterically regulate interdomain communication in NHERF1, leading to phosphorylation of Ser²⁹⁰ in its EBD and concurrent disassembly of NPT2A from

Phosphoserine 162 of PDZ2 orchestrates binding to GRK6A

PDZ1 (Fig. 7), which is required for inhibition of phosphate transport (16). Allosteric networks and allosteric communication are essential regulators of PDZ-containing multidomain protein conformational changes and function (44, 45).

In summary, the present findings provide strong evidence that GRK6A is vital for hormone-sensitive phosphate uptake. Our biochemical results demonstrate that phosphorylation of Ser¹⁶² regulates the interaction between PDZ2 and the GRK6A C-terminal PDZ-binding motif. This observation is corroborated by binding affinities and MD simulations. Based on these outcomes, we propose an extended model of PTH-sensitive phosphate transport where NHERF1 PDZ1 associates with NPT2A and serves as a functional platform for hormone-regulated phosphate transport, whereas PDZ2 targets GRK6A via PKC α phosphorylation of Ser¹⁶² and works as a regulatory domain. GRK6A and PKC α represent two complementary and parallel pathways of PTH signaling. PTH-induced phosphorylation of Ser¹⁶² may be part of a selectivity mechanism that allows NHERF1 PDZ domains to discriminate between target ligands.

Experimental procedures

Cell culture and transfection

Parental OK or NHERF1-deficient (OKH) cells (4) were grown in Dulbecco's modified Eagle's medium/Ham's F-12 50:50 medium (Mediatech, 10-090-CV) supplemented with 10% fetal bovine serum and 1% pen/strep.

Cells were transfected with the indicated plasmids using jetPRIME (Polyplus) or Lipofectamine 3000 (Invitrogen) according to the manufacturer's instructions. Stable OKH cells expressing FLAG-NHERF1, FLAG-NHERF1 constructs or FLAG-NHERF1 mutants, and HA-GRK6A were prepared by transferring cells and then selecting for stable expression with puromycin or G418 and then subcloning by limiting dilution.

Preparation of endogenous NHERF1 and NHERF1 constructs

WT or mutant NHERF1 tagged with FLAG was prepared as described (16).

Phosphate uptake

OKH cells were seeded on 12-well plates and 24 h later were transfected with FLAG-NHERF1 (WT or mutant) using jetPRIME, as indicated. After 48 h, the cells were serum-starved overnight. The next day, the transfected cells were treated with 100 nM PTH(1–34) or water (vehicle) in cell culture media for 2 h. The hormone-supplemented medium was aspirated, and the wells were washed 3 times with 1 ml of Na-replete buffer (140 mM NaCl, 4.8 mM KCl, 1.2 mM MgSO₄, 0.1 mM KH₂PO₄, 10 mM HEPES, pH 7.4). The cells were incubated with 1 μ Ci of ³²P orthophosphate (PerkinElmer, NEX053) in 1 ml of the Na-replete wash buffer for 10 min. Phosphate uptake was terminated by placing the plate on ice and rinsing the cells three times in Na-free wash buffer (140 mM N-methyl-D-glucamine, 4.8 mM KCl, 1.2 mM MgSO₄, 0.1 mM KH₂PO₄, 10 mM HEPES, pH 7.4). The cells in each well were extracted using 500 μ l 1% Triton X100 (Sigma Cat X100) in

water overnight at 4 °C. A 250 μ l aliquot was counted in a Beckmann Coulter LS6500 liquid scintillation counter. Data were normalized, where 100% was defined as cpm of phosphate uptake under control conditions.

siRNA knockdown

siRNA for Grk6a knockdown was designed by and purchased from Integrated DNA Technologies (IDT). The siRNA was transfected into OK cells using LipoJet (100468, SignaGen Laboratories). Cells were transfected on 60 mm dishes. Forty-eight hours after transfection, the cells were trypsinized and passaged onto 12-well plates for phosphate-uptake assays. Protein lysates were extracted from a 100 μ l aliquot of these cells to assess by immunoblot the extent of Grk6a knockdown.

Immunoprecipitation and immunoblotting

Transfected OKH cells were lysed with 1% Nonidet P-40 (50 mM Tris, 150 mM NaCl, 5 mM EDTA, 1% Nonidet P-40) supplemented with protease inhibitor mixture I (Calbiochem). Lysis was performed for 15 min on ice. Solubilized materials were resolved on 10% SDS-polyacrylamide gels and transferred to Immobilon-P membranes (Millipore) using the semidry method (Bio-Rad). Membranes were blocked overnight at 4 °C with 5% nonfat dried milk in Tris-buffered saline plus Tween 20 (TBST) and incubated with the indicated primary antibodies overnight at 4 °C. The membranes were washed four times for 10 min in TBST and then incubated with goat anti-rabbit IgG or anti-mouse IgG conjugated to horseradish peroxidase at a 1:5000 dilution for 1 h at room temperature. Membranes were washed 4 times for 10 min in TBST. Protein bands were detected by Luminol-based enhanced chemiluminescence (EMD Millipore WBKLS0500).

Recombinant constructs and protein purification

The expression plasmids pET16-N1P1 encoding PDZ1 (1–140) and pET16-N1P2 encoding PDZ2 (133–300 aa) of NHERF1 were kindly provided by Dr Dale F. Mierke (Department of Chemistry, Dartmouth College, Hanover, NH). Plasmid fidelity was confirmed by DNA sequencing (ABI PRISM 377, Applied Biosystems) and subsequent sequence alignment (NCBI BLAST) with human NHERF1 (GenBank AF015926) to ensure the accuracy of the constructs. Recombinant proteins were expressed in *E. coli* BL21 (DE3) cells (Novagen) and purified using Ni-NTA-agarose (Qiagen) (46). Full-length NHERF1 and NHERF1 constructs were generated in the laboratory. The resulting proteins were divided into aliquots and stored in the phosphate buffer (25 mM NaH₂PO₄, 10 mM NaCl, pH 7.4) at –80 °C until used for FA experiments. The -GYGF- core-binding mutations were introduced in PDZ1 or PDZ2 of full-length NHERF1 (N1): N1P1: ²³GYGF^{26/23}GAGA²⁶; N1P2: ¹⁶³GYGF^{166/163}GAGA¹⁶⁶; and N1P1P2: ²³GYGF²⁶ ¹⁶³GYGF^{166/23}GAGA²⁶ ¹⁶³GAGA¹⁶⁶, using the QuikChange site-directed mutagenesis kit. All construct sequences were confirmed by DNA sequencing.

Substitution of Tyr²⁴/Tyr¹⁶⁴ and Phe²⁶/Phe¹⁶⁶ by Ala in the carboxylate binding site of full-length NHERF1 eliminates

canonical hydrophobic interactions and therefore significantly decreases binding affinity of PDZ1–GAGA or PDZ2–GAGA to bind PDZ-binding motifs of targets compared with unmodified PDZ domains. NHERF1 with modified carboxylate-binding sites may serve as a suitable model to estimate the interaction between full-length NHERF1 (1–358 aa) where one PDZ domain is available for binding, whereas the other PDZ domain has a negligible binding affinity for binding the target.

Generation of pSer¹⁶²–PDZ2

Chemically competent *E. coli* BL21 Δ SerB (AddGene #34929) cells were cotransformed with pCDF-1b Nherf1 PDZ2 (133–300) Ser¹⁶²TAG 6xHis and pKW2 EF-Sep (25) and plated on LB agar plates containing 100 μ g/ml spectinomycin and 25 μ g/ml chloramphenicol. Precultures were grown overnight at 30 °C and diluted to an absorbance of 600 nm of 0.1 in fresh LB media containing antibiotics and grown at 37 °C to an absorbance of 600 nm of 0.5. Protein expression was induced by addition of 0.5 mM IPTG, and the medium was supplemented with 1 mM *O*-phospho-L-serine (Sigma). The protein was expressed at 30 °C for 4 h, shaking at 150 rpm. Cells were harvested by centrifugation, 10,000g, at 4 °C for 10 min. The cell pellet was lysed in 4 ml/g pellet B-PER Bacterial Extraction Reagent supplemented with DNase and protease inhibitor and spun down by centrifugation, 30,000g, at 4 °C for 30 min. The supernatant was loaded on a pre-equilibrated (50 mM Tris, 150 mM NaCl, 2 mM β -mercaptoethanol, pH 8) HisTrap Ni²⁺ column (GE Healthcare), which was extensively washed after loading. The protein was eluted using an ÄKTAExplorer 100 Air system (GE Healthcare) with a gradient of imidazole (50 mM Tris, 150 mM NaCl, 100 mM imidazole, 2 mM β -mercaptoethanol, pH 8). The protein was further purified by gel filtration (50 mM Tris, 150 mM NaCl, 2 mM β -mercaptoethanol, pH 8). The protein concentration was determined by 280 nm absorbance on a Nanodrop 1000 (Thermo Fisher Scientific). The purified protein was analyzed by ESI-LC-MS (Agilent) and Acquity UPLC (Waters) for the identification of mass and purity, respectively. The various purification steps were followed by SDS-PAGE.

CD

The secondary structure of NHERF1 PDZ2 pSer¹⁶² 6x His was visualized by CD in 50 mM NaPi buffer, pH 8. All recordings were made using a Jasco J1500 CD spectrometer (Jasco) in 1 mm quartz cuvettes (BioLab). Recordings were carried out on 10 μ M protein samples at 25 °C, and at 95 °C immediately followed by a 25 °C scan to assess the refolding. Three accumulated scans for each temperature were acquired for 260 to 190 nm and analyzed in Prism (GraphPad).

Peptides

A FITC-labeled human GRK6A C-terminal 22 amino acid peptide, GRK6Act-22, was synthesized by LifeTein. The WT and FITC-labeled peptides were dissolved and serially diluted in PBS (pH 7.4).

FA saturation binding

Solution phase direct binding assays were performed to measure binding affinity (K_D) between NHERF1, NHERF1 constructs (N1P1-GAGA and N1P2-GAGA), isolated PDZ domain, pSer¹⁶²-PDZ2 or S¹⁶²A-PDZ2, and FITC-GRK6Act-22 after the previously reported protocols for NHERF1 PDZ domains (28, 29, 39). All measurements were performed in PBS (pH 7.4) supplemented with 0.1% BSA and 1-mM DTT by applying increasing amounts of the recombinant proteins to a fixed concentration of the FITC-labeled peptide (0.4–1.0 μ M). FA assays were run on a 96-well format and performed in triplicate in three to five independent experiments. Polarized fluorescence intensities were measured at 23 °C with a PerkinElmer Wallac VICTOR3 multilabel counter using excitation and emission wavelengths of 485 nm and 535 nm, respectively. Experimental data were analyzed using Prism (GraphPad). All measurements are reported as FA rather than polarization. FA was computed using Equation 1 from the measured fluorescence emission intensities that are polarized parallel (I_{\parallel}) and perpendicular (I_{\perp}) to the plane of the incident light (47):

$$r = I_x - I_{\perp} / I_x + 2I_{\perp} \quad (3)$$

The equilibrium dissociation constant (K_D) for the interaction between the indicated PDZ domain and labeled peptide was determined by fitting the FA data to a quadratic equation (47) as described (28).

Model setup and molecular docking

The structures of the NHERF1 PDZ1 and PDZ2 domains (residues 13–91 and 148–240, respectively) were derived from our previous MD simulations (39, 48). The residues forming the binding pocket of PDZ1 or PDZ2 (14, 48) were selected indicated for molecular docking. GRK6Act-9 was generated by PyMol (49) with the sequence corresponding to residues 0 to –8 numbered according to the convention as described earlier. The length of the peptide was designed according to our and other studies demonstrating the effect of upstream residues up to –8 position on PDZ-ligand interactions (29, 39, 50). After a short equilibration run (100 ps), a random conformation of GRK6Act-9 was selected for molecular docking. Docking was performed between GRK6Act-9 and PDZ1, PDZ2, or pSer¹⁶²-PDZ2 using ZDOCK (version 3.0.2) (27). Several ZDOCK runs were performed to entertain substantial possible structures. Because the conformational changes between the bound and unbound PDZ1 or PDZ2 is modest (28, 39, 48), it is appropriate to use rigid-body algorithms such as ZDOCK (27). The top ten models from each ZDOCK run were downloaded and viewed by PyMol (49). All models were examined using the following criteria: (i) The C-terminal Leu⁰ of GRK6A (Leu⁵⁷⁶) is inserted in the PDZ domain hydrophobic pocket between the α 2 helix and the β 2 sheet; (ii) the docked peptide is in the antiparallel orientation to the

Phosphoserine 162 of PDZ2 orchestrates binding to GRK6A

binding pocket of the PDZ domain; (iii) the extreme C terminus of the docked peptide is not involved in contacts with any part of PDZ domain except the PDZ binding pocket. pSer¹⁶²-PDZ2 was built by replacing the hydrogen atom of the serine residue by a phosphoryl group ($-\text{PO}_3^{-2}$) using the Leap module of AMBER16 (51). The coordinate file for the phosphate group of pSer¹⁶² was renamed to phosphoserine. The best docking models for PDZ1-GRK6Act-9, PDZ2-GRK6Act-9, and pSer¹⁶²-PDZ2-GRK6Act-9 derived from the above criteria were selected for MD simulations. Files required for MD simulations were prepared by the Leap module of AMBER16 (51). Then, PDZ1/2-GRK6Act-9 complexes were solvated with TIP3P water molecules (52) in a periodically replicated box, neutralized with Na^+ , and energy-minimized over 500 steps including 100 steps of steepest descent minimization using the AMBER16 pmemd module (51).

In addition, the carboxylate-binding site (-GYGF-) in pSer¹⁶²-PDZ2 was replaced by the GAGA sequence, and MD simulations (100 ns) were performed as described for PDZ1/PDZ2-GRK6A. A model established using the Leap module of AMBER16 (51).

MD simulations

MD simulations were performed using the AMBER16 package with the AMBER force field (ff99SB) and phosaa10 (51) to describe pSer¹⁶². The simulation details, equilibration, and production simulations, except for the length, were set according to our previous studies (28, 39, 48). In brief, the short runs (0.8 ns) were executed under the NPT ensemble (constant number of particles [N], pressure [P], and temperature [T]) to equilibrate the water molecules. During this equilibration, harmonic restraints were applied to the ligand residues and methodically lowered from $k_s = 10 \text{ kcal/mol}/\text{\AA}^2$ to $0.1 \text{ kcal/mol}/\text{\AA}^2$. Then, equilibration runs (50–70 ns) were continued under the NVT ensemble (constant number of particles [N], volume [V], and temperature [T]) with harmonic restraints $k_s = 0.5 \text{ kcal/mol}/\text{\AA}^2$ or $0.1 \text{ kcal/mol}/\text{\AA}^2$ applied to the ligand. Upon completion of equilibration, production simulations were conducted at 300 K using the canonical NVT ensemble with configurations saved every 2 fs for analysis. Weak harmonic restraints ($k_s = 0.1 \text{ kcal/mol}/\text{\AA}^2$) were applied to the N-terminal backbone atoms of the ligand and PDZ domain to prevent diffusion from the simulation box. MD simulations were performed for 150 ns each including the equilibration phase. The equilibration phase and production simulations were monitored by computing the RMSD of the C α atoms from their initial positions (not presented here).

Data analysis

Results were analyzed using Prism 8.2.1 software (GraphPad). Results represent the mean \pm SE of $n \geq 3$ independent experiments, unless indicated otherwise, and were compared by analysis of variance (ANOVA) with

Bonferroni *post hoc* testing. *p* Values <0.05 were considered statistically significant.

Data availability

Data for all tables are contained within the article. Data for all figures are available from Tatyana Mamonova (tbm7@pitt.edu).

Supporting information—This article contains [supporting information](#).

Acknowledgments—We are grateful to Dr Qiangmin Zhang for preparing NHERF1 constructs used here. Dr Dale F. Mierke kindly provided pET16-N1P1 encoding PDZ1 (1–140) and pET16-N1P2 encoding PDZ2 (133–300 aa) of NHERF1. This work was supported by National Institutes of Health grant R01DK105811. The content is solely the responsibility of the authors and does not necessarily represent the official views of the National Institutes of Health.

Author contributions—M. V. -P., S. B., T. M., and W. B. S investigation; T. M., P. A. F., and K. S. methodology; T. M., P. A. F., M. V. -P., and K. S. writing-original draft; T. M. and P. A. F. writing-review and editing; T. M., P. A. F., M. V.-P., and K. S. formal analysis; T. M. and M. V.-P. visualization; T. M., P. A. F., and K. S. conceptualization; P. A. F. funding acquisition; T. M. and P. A. F. supervision; T. M. project administration.

Conflict of interest—The authors declare that they have no conflicts of interest with the contents of this article.

Abbreviations—The abbreviations used are: CFTR, cystic fibrosis transmembrane conductance regulator; C-terminal, carboxy-terminal; EBD, ezrin-binding domain; FA, fluorescence anisotropy; GRK6A, G protein-coupled receptor kinase 6AGRK6Act-22, ⁵⁵³QRLFSRQDCCGNCSEELPTRL⁵⁷⁶; GRK6Act-9, ⁵⁶⁸SEELPTRL⁵⁷⁶; NHERF1, Na^+/H^+ -exchanger regulatory factor-1; NPT2A, type II sodium-dependent phosphate cotransporter; OK cells, opossum kidney cells; OKH, opossum kidney clone H; pSer¹⁶², phosphorylated Ser¹⁶²; PTH, parathyroid hormone; TBST, Tris-buffered saline plus Tween 20.

References

1. Donowitz, M., Cha, B., Zachos, N. C., Brett, C. L., Sharma, A., Tse, C. M., and Li, X. (2005) NHERF family and NHE3 regulation. *J. Physiol.* **567**, 3–11
2. Ardura, J. A., and Friedman, P. A. (2011) Regulation of G protein-coupled receptor function by Na^+/H^+ exchange regulatory factors. *Pharmacol. Rev.* **63**, 882–900
3. Romero, G., von Zastrow, M., and Friedman, P. A. (2011) Role of PDZ proteins in regulating trafficking, signaling, and function of GPCRs: Means, motif, and opportunity. *Adv. Pharmacol.* **62**, 279–314
4. Wang, B., Means, C. K., Yang, Y. M., Mamonova, T., Bisello, A., Altschuler, D. L., Scott, J. D., and Friedman, P. A. (2012) Ezrin-anchored protein kinase A coordinates phosphorylation-dependent disassembly of a NHERF1 ternary complex to regulate hormone-sensitive phosphate transport. *J. Biol. Chem.* **287**, 24148–24163
5. Karim, Z., Gerard, B., Bakouh, N., Alili, R., Leroy, C., Beck, L., Silve, C., Planelles, G., Urena-Torres, P., Grandchamp, B., Friedlander, G., and

- Prie, D. (2008) NHERF1 mutations and responsiveness of renal parathyroid hormone. *N. Engl. J. Med.* **359**, 1128–1135
6. Gordon, R. J., Li, D., Doyle, D., Zaritsky, J., and Levine, M. A. (2020) Digenic heterozygous mutations in SLC34A3 and SLC34A1 cause dominant hypophosphatemic rickets with hypercalciuria. *J. Clin. Endocrinol. Metab.* **105**, 2392–2400
 7. Kang, S. J., Lee, R., and Kim, H. S. (2019) Infantile hypercalcemia with novel compound heterozygous mutation in SLC34A1 encoding renal sodium-phosphate cotransporter 2a: A case report. *Ann. Pediatr. Endocrinol. Metab.* **24**, 64–67
 8. Shenolikar, S., Voltz, J. W., Minkoff, C. M., Wade, J. B., and Weinman, E. J. (2002) Targeted disruption of the mouse NHERF-1 gene promotes internalization of proximal tubule sodium-phosphate cotransporter type IIa and renal phosphate wasting. *Proc. Natl. Acad. Sci. U. S. A.* **99**, 11470–11475
 9. Morales, F. C., Takahashi, Y., Kreimann, E. L., and Georgescu, M. M. (2004) Ezrin-radixin-moesin (ERM)-binding phosphoprotein 50 organizes ERM proteins at the apical membrane of polarized epithelia. *Proc. Natl. Acad. Sci. U. S. A.* **101**, 17705–17710
 10. Hernando, N., Deliot, N., Gisler, S. M., Lederer, E., Weinman, E. J., Biber, J., and Murer, H. (2002) PDZ-domain interactions and apical expression of type IIa Na/P_i cotransporters. *Proc. Natl. Acad. Sci. U. S. A.* **99**, 11957–11962
 11. Weinman, E. J., Steplock, D., Shenolikar, S., and Biswas, R. (2011) Fibroblast growth factor-23-mediated inhibition of renal phosphate transport in mice requires sodium-hydrogen exchanger regulatory factor-1 (NHERF-1) and synergizes with parathyroid hormone. *J. Biol. Chem.* **286**, 37216–37221
 12. Karthikeyan, S., Leung, T., and Ldias, J. A. A. (2001) Structural basis of the Na⁺/H⁺ exchanger regulatory factor PDZ1 interaction with the carboxyl-terminal region of the cystic fibrosis transmembrane conductance regulator. *J. Biol. Chem.* **276**, 19683–19686
 13. Karthikeyan, S., Leung, T., Birrane, G., Webster, G., and Ldias, J. A. A. (2001) Crystal structure of the PDZ1 domain of human Na⁺/H⁺ exchanger regulatory factor provides insights into the mechanism of carboxyl-terminal leucine recognition by class I PDZ domains. *J. Mol. Biol.* **308**, 963–973
 14. Karthikeyan, S., Leung, T., and Ldias, J. A. (2002) Structural determinants of the Na⁺/H⁺ exchanger regulatory factor interaction with the β₂ adrenergic and platelet-derived growth factor receptors. *J. Biol. Chem.* **277**, 18973–18978
 15. Hall, R. A., Spurney, R. F., Premont, R. T., Rahman, N., Blitzer, J. T., Pitcher, J. A., and Lefkowitz, R. J. (1999) G protein-coupled receptor kinase 6A phosphorylates the Na⁺/H⁺ exchanger regulatory factor via a PDZ domain-mediated interaction. *J. Biol. Chem.* **274**, 24328–24334
 16. Zhang, Q., Xiao, K., Paredas, J. M., Mamonova, T., Sneddon, W. B., Liu, H., Wang, D., Li, S., McGarvey, J. C., Uehling, D., Al-awar, R., Josef, J., Alphonse, F., Orte, A., and Friedman, P. A. (2019) Parathyroid hormone initiates dynamic NHERF1 phosphorylation cycling and conformational changes that regulate NPT2A-dependent phosphate transport. *J. Biol. Chem.* **294**, 4546–4571
 17. Raghuram, V., Hormuth, H., and Foskett, J. K. (2003) A kinase-regulated mechanism controls CFTR channel gating by disrupting bivalent PDZ domain interactions. *Proc. Natl. Acad. Sci. U. S. A.* **100**, 9620–9625
 18. Li, J. Q., Poulikakos, P. I., Dai, Z. P., Testa, J. R., Callaway, D. J. E., and Bu, Z. M. (2007) Protein kinase c phosphorylation disrupts Na⁺/H⁺ exchanger regulatory factor 1 autoinhibition and promotes cystic fibrosis transmembrane conductance regulator macromolecular assembly. *J. Biol. Chem.* **282**, 27086–27099
 19. Khundmiri, S. J., Weinman, E. J., Steplock, D., Cole, J., Ahmad, A., Baumann, P. D., Barati, M., Rane, M. J., and Lederer, E. (2005) Parathyroid hormone regulation of Na⁺,K⁺-ATPase requires the PDZ 1 domain of sodium hydrogen exchanger regulatory factor-1 in opossum kidney cells. *J. Am. Soc. Nephrol.* **16**, 2598–2607
 20. Voltz, J. W., Brush, M., Sikes, S., Steplock, D., Weinman, E. J., and Shenolikar, S. (2007) Phosphorylation of PDZ1 domain attenuates NHERF-1 binding to cellular targets. *J. Biol. Chem.* **282**, 33879–33887
 21. Weinman, E. J., Steplock, D., Shenolikar, S., and Blanpied, T. A. (2011) Dynamics of PTH-induced disassembly of Npt2a/NHERF-1 complexes in living OK cells. *Am. J. Physiol. Ren. Physiol.* **300**, F231–235
 22. Pouyssegur, J., Sardet, C., Franchi, A., L'Allemain, G., and Paris, S. (1984) A specific mutation abolishing Na⁺/H⁺ antiport activity in hamster fibroblasts precludes growth at neutral and acidic pH. *Proc. Natl. Acad. Sci. U. S. A.* **81**, 4833–4837
 23. Staudinger, J., Lu, J., and Olson, E. N. (1997) Specific interaction of the PDZ domain protein PICK1 with the COOH terminus of protein kinase C-α. *J. Biol. Chem.* **272**, 32019–32024
 24. Biber, J., Malmstrom, K., Reshkin, S., and Murer, H. (1990) Phosphate transport in established renal epithelial cell lines. *Methods Enzymol.* **191**, 494–505
 25. Rogerson, D. T., Sachdeva, A., Wang, K., Haq, T., Kazlauskaitė, A., Hancock, S. M., Huguenin-Dezot, N., Muqit, M. M., Fry, A. M., Bayliss, R., and Chin, J. W. (2015) Efficient genetic encoding of phosphoserine and its nonhydrolyzable analog. *Nat. Chem. Biol.* **11**, 496–503
 26. Pedersen, S. W., Albertsen, L., Moran, G. E., Levesque, B., Pedersen, S. B., Bartels, L., Wapenaar, H., Ye, F., Zhang, M., Bowen, M. E., and Stromgaard, K. (2017) Site-specific phosphorylation of PSD-95 PDZ domains reveals fine-tuned regulation of protein-protein interactions. *ACS Chem. Biol.* **12**, 2313–2323
 27. Pierce, B. G., Wiehe, K., Hwang, H., Kim, B. H., Vreven, T., and Weng, Z. (2014) ZDOCK server: Interactive docking prediction of protein-protein complexes and symmetric multimers. *Bioinformatics* **30**, 1771–1773
 28. Mamonova, T., Zhang, Q., Khajeh, J. A., Bu, Z., Bisello, A., and Friedman, P. A. (2015) Canonical and noncanonical sites determine NPT2A binding selectivity to NHERF1 PDZ1. *PLoS One* **10**, e0129554
 29. Cushing, P. R., Fellows, A., Villone, D., Boisguerin, P., and Madden, D. R. (2008) The relative binding affinities of PDZ partners for CFTR: A biochemical basis for efficient endocytic recycling. *Biochemistry* **47**, 10084–10098
 30. Bhattacharya, S., Dai, Z. P., Li, J. Q., Baxter, S., Callaway, D. J. E., Cowburn, D., and Bu, Z. M. (2010) A conformational switch in the scaffolding protein NHERF1 controls autoinhibition and complex formation. *J. Biol. Chem.* **285**, 9981–9994
 31. Bhattacharya, S., Ju, J. H., Orlova, N., Khajeh, J. A., Cowburn, D., and Bu, Z. M. (2013) Ligand-induced dynamic changes in extended PDZ domains from NHERF1. *J. Mol. Biol.* **425**, 2509–2528
 32. Mahon, M. J. (2009) The parathyroid hormone 1 receptor directly binds to the FERM domain of ezrin, an interaction that supports apical receptor localization and signaling in LLC-PK1 cells. *Mol. Endocrinol.* **23**, 1691–1701
 33. Cunningham, R., E, X., Steplock, D., Shenolikar, S., and Weinman, E. J. (2005) Defective PTH regulation of sodium-dependent phosphate transport in NHERF-1^{-/-} renal proximal tubule cells and wild-type cells adapted to low-phosphate media. *Am. J. Physiol. Ren. Physiol.* **289**, F933–938
 34. Ernst, A., Appleton, B. A., Ivarsson, Y., Zhang, Y., Gfeller, D., Wiesmann, C., and Sidhu, S. S. (2014) A structural portrait of the PDZ domain family. *J. Mol. Biol.* **426**, 3509–3519
 35. Hall, R. A., and Lefkowitz, R. J. (2002) Regulation of G protein-coupled receptor signaling by scaffold proteins. *Circ. Res.* **91**, 672–680
 36. Salyer, S., Lesousky, N., Weinman, E. J., Clark, B. J., Lederer, E. D., and Khundmiri, S. J. (2011) Dopamine regulation of Na⁺-K⁺-ATPase requires the PDZ-2 domain of sodium hydrogen regulatory factor-1 (NHERF-1) in opossum kidney cells. *Am. J. Physiol. Cell Physiol.* **300**, C425–434
 37. Awadia, S., Huq, F., Arnold, T. R., Goicoechea, S. M., Sun, Y. J., Hou, T., Kreider-Letterman, G., Massimi, P., Banks, L., Fuentes, E. J., Miller, A. L., and Garcia-Mata, R. (2019) SGEF forms a complex with Scribble and Dlg1 and regulates epithelial junctions and contractility. *J. Cell Biol.* **218**, 2699–2725
 38. Martin, E. R., Barbieri, A., Ford, R. C., and Robinson, R. C. (2020) *In vivo* crystals reveal critical features of the interaction between cystic fibrosis transmembrane conductance regulator (CFTR) and the PDZ2 domain of Na(+)/H(+) exchange cofactor NHERF1. *J. Biol. Chem.* **295**, 4464–4476

Phosphoserine 162 of PDZ2 orchestrates binding to GRK6A

39. Mamonova, T., Zhang, Q., Chandra, M., Collins, B. M., Sarfo, E., Bu, Z., Xiao, K., Bisello, A., and Friedman, P. A. (2017) Origins of PDZ binding specificity. A computational and experimental study using NHERF1 and the parathyroid hormone receptor. *Biochemistry* **56**, 2584–2593
40. Weinman, E. J., Steplock, D., Zhang, Y., Biswas, R., Bloch, R. J., and Shenolikar, S. (2010) Cooperativity between the phosphorylation of Thr95 and Ser77 of NHERF-1 in the hormonal regulation of renal phosphate transport. *J. Biol. Chem.* **285**, 25134–25138
41. Amacher, J. F., Cushing, P. R., Brooks, L., Boisguerin, P., and Madden, D. R. (2014) Stereochemical preferences modulate affinity and selectivity among five PDZ domains that bind CFTR: Comparative Structural and Sequence Analyses. *Structure* **22**, 82–93
42. Alshafe, W., Chappe, F. G., Li, M., Anini, Y., and Chappe, V. M. (2014) VIP regulates CFTR membrane expression and function in Calu-3 cells by increasing its interaction with NHERF1 and P-ERM in a VPAC1- and PKCepsilon-dependent manner. *Am. J. Physiol. Cell Physiol.* **307**, C107–119
43. Toto, A., Mattei, A., Jemth, P., and Gianni, S. (2017) Understanding the role of phosphorylation in the binding mechanism of a PDZ domain. *Protein Eng. Des. Sel.* **30**, 1–5
44. Laursen, L., Karlsson, E., Gianni, S., and Jemth, P. (2020) Functional interplay between protein domains in a supramolecular structure involving the postsynaptic density protein PSD-95. *J. Biol. Chem.* **295**, 1992–2000
45. Laursen, L., Kliche, J., Gianni, S., and Jemth, P. (2020) Supertertiary protein structure affects an allosteric network. *Proc. Natl. Acad. Sci. U. S. A.* **117**, 24294–24304
46. Wang, B., Yang, Y. M., and Friedman, P. A. (2008) Na/H exchange regulatory factor 1, a novel AKT-associating protein, regulates extracellular signal-regulated kinase signaling through a B-Raf-mediated pathway. *Mol. Biol. Cell* **19**, 1637–1645
47. Roehrl, M. H. A., Wang, J. Y., and Wagner, G. (2004) A general framework for development and data analysis of competitive high-throughput screens for small-molecule inhibitors of protein - protein interactions by fluorescence polarization. *Biochemistry* **43**, 16056–16066
48. Mamonova, T., Kurnikova, M., and Friedman, P. A. (2012) Structural basis for NHERF1 PDZ domain binding. *Biochemistry* **51**, 3110–3120
49. Janson, G., Zhang, C., Prado, M. G., and Paiardini, A. (2017) PyMod 2.0: improvements in protein sequence-structure analysis and homology modeling within PyMOL. *Bioinformatics* **33**, 444–446
50. Clairfeuille, T., Mas, C., Chan, A. S., Yang, Z., Tello-Lafoz, M., Chandra, M., Widagdo, J., Kerr, M. C., Paul, B., Merida, I., Teasdale, R. D., Pavlos, N. J., Anggono, V., and Collins, B. M. (2016) A molecular code for endosomal recycling of phosphorylated cargos by the SNX27-retromer complex. *Nat. Struct. Mol. Biol.* **23**, 921–932
51. Case, D. A., Betz, R. M., Cerutti, D. S., Cheatham, I. E., T., Darden, T. A., Duke, R. E., Giese, T. J., Gohlke, H., Goetz, A. M., Homeyer, N., Izadi, S., Janowski, P., Kaus, J., Kovalenko, A., *et al.* (2016) *Amber 2016*, University of California, San Francisco, CA
52. Jorgensen, W. L., Chandrasekhar, J., Madura, J. D., Impey, R. W., and Klein, M. L. (1983) Comparison of simple potential functions for simulating liquid water. *J. Chem. Phys.* **79**, 926–935